



Avalanche breakdown and quenching in Ge SPAD using 3D Monte Carlo simulation

Philippe Dollfus, Jérôme Saint-Martin, T. Cazimajou, R. Helleboid, A. Pilotto, D. Rideau, A. Bournel, Marco G. Pala

► To cite this version:

Philippe Dollfus, Jérôme Saint-Martin, T. Cazimajou, R. Helleboid, A. Pilotto, et al.. Avalanche breakdown and quenching in Ge SPAD using 3D Monte Carlo simulation. Solid-State Electronics, 2022, 194, pp.108361. 10.1016/j.sse.2022.108361 . hal-03793955

HAL Id: hal-03793955

<https://cnrs.hal.science/hal-03793955>

Submitted on 18 Nov 2022

HAL is a multi-disciplinary open access archive for the deposit and dissemination of scientific research documents, whether they are published or not. The documents may come from teaching and research institutions in France or abroad, or from public or private research centers.

L'archive ouverte pluridisciplinaire **HAL**, est destinée au dépôt et à la diffusion de documents scientifiques de niveau recherche, publiés ou non, émanant des établissements d'enseignement et de recherche français ou étrangers, des laboratoires publics ou privés.

Avalanche breakdown and quenching in Ge SPAD using 3D Monte Carlo simulation

P. Dollfus¹, J. Saint-Martin¹, T. Cazimajou¹, R. Helleboid^{1,2}, A. Pilotto¹,
D. Rideau², A. Bournel¹ and M. Pala¹

¹ Université Paris-Saclay, CNRS, Centre de Nanosciences et de Nanotechnologies, Palaiseau, France, email: philippe.dollfus@universite-paris-saclay.fr

² STMicroelectronics, Crolles, France

Keywords - Avalanche breakdown; particle Monte Carlo method; avalanche photodiode

1. Abstract

A Ge-based single-photon-avalanche-diode (SPAD) is investigated by using self-consistent 3-D Monte Carlo simulation including the presence of a passive quenching circuit. This approach of transport allows us to capture all stochastic features of carrier transport and SPAD operation. We analyze particularly the probabilistic character of the quenching mechanism and its dependence on the parameters (resistance and capacitance) of the passive quenching circuit.

2. Introduction

The market of single-photon avalanche diodes (SPADs) is dominated by Si devices but SPADs made of, or including, germanium are likely to provide some advantages for specific applications. Indeed, due to smaller bandgap, Ge devices should be sensitive to wavelengths larger than 1400 nm (eye-safety devices) and able to operate under smaller bias voltage than their Si counterparts (reduced power consumption). They hold great promise, insofar as Ge is compatible with Si technology.

In terms of theoretical investigation of device design, the full SPAD operation in the presence of quenching circuit has mainly been discussed so far on the basis of compact modeling [1] [2]. Computationally efficient Verilog-A model and TCAD mixed-mode simulation can be used as well [3]. To go beyond these strongly simplified methods, we have developed a particle Monte Carlo (MC) model self-consistently coupled to a 3D Poisson solver and able to include the passive quenching circuit in a mixed-mode approach [4]. In the present work, this model is used to study the main features of operation of a Ge SPAD, including in particular the statistics of quenching. The particle Monte Carlo approach of solving the Boltzmann transport equation is indeed well suited for such investigation since it naturally includes all stochastic features of carrier transport.

3. Model and simulated device

The simulated structure is similar to that previously used for the Si SPAD studied in [4]. It consists in a Ge PN junction of length $L = 1300$ nm and square cross section of width $W = 300$ nm. It is connected in series with a passive quenching RC circuit. The diode has a doping profile $N_A = 6 \times 10^{17} \text{ cm}^{-3}$ and $N_D = 6.35 \times 10^{17} \text{ cm}^{-3}$, with a quasi-linear transition region of 900 nm-long. A voltage V_{BIAS} is applied between the terminals of the circuit composed by the SPAD and quenching circuit in series.

The 3D particle Monte Carlo code used here is self-consistently coupled to the Poisson's equation [5]. In this model the analytic conduction band of Ge is made of four ellipsoidal L valleys, i.e. eight half valleys in the

first Brillouin zone, one spherical Γ valley and six ellipsoidal Δ valleys [6], while the heavy and light hole bands are spherical and non-parabolic, with the room-temperature effective masses determined in [7].

To describe impact ionization processes, we implemented Keldysh like formulations of ionization rates [8] with parameters adjusted to fit the experimental field dependence of ionization coefficients, as shown in Fig. 1.

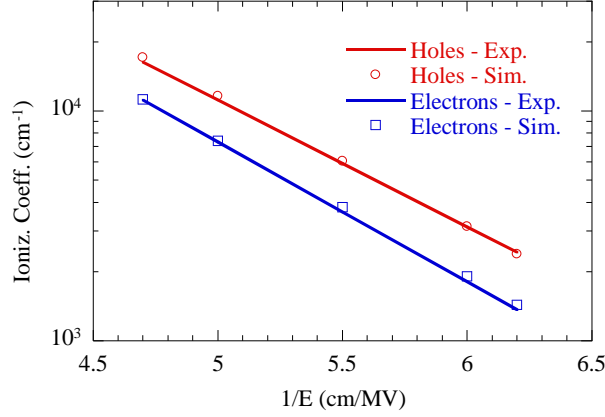


Figure 1. Ionization coefficient in Ge as a function of inverse electric field. Comparison between (lines) experimental data [9] and (symbols) simulation.

The connection of the SPAD with the passive (R_Q, C_Q) quenching circuit is made in a mixed-mode approach, as described in [4]. At each time step of Poisson's equation solution the SPAD voltage V_{SPAD} is updated according to the current in the device (calculated using the Ramo-Shockley theorem [10]) and the quenching circuit elements. The initial single photon absorption is simulated by generating the first electron-hole (e-h) pair with energy and momentum randomly selected assuming thermal equilibrium distribution.

4. Results

The internal capacitance $C_{SPAD} = 30.9$ aF and resistance $R_{SPAD} = 23.5$ k Ω have been deduced from the I - V and Q - V characteristics (see Fig. 2), together with the avalanche breakdown voltage $V_{BD} = 8.6$ V. Due to smaller bandgap of Ge (0.76 eV) than in Si (1.12 eV), this breakdown voltage is significantly lower than that of 15.3 V in the similar Si SPAD [4], which allows us to use a small bias voltage $V_{BIAS} = 11$ V instead of typically 17-20 V in Si devices.

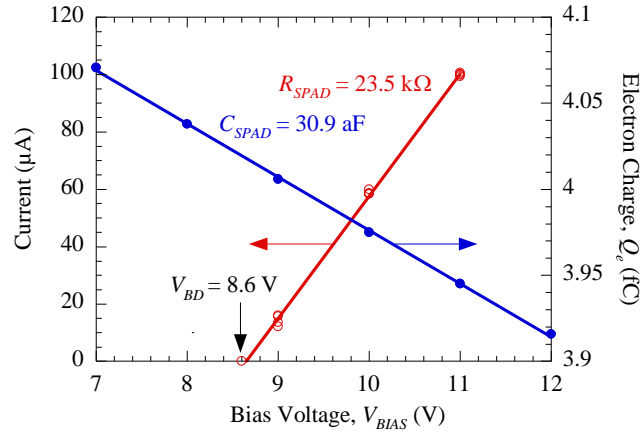


Figure 2. Avalanche current (red) and steady-state electron charge (blue) inside the device as a function of bias voltage.

The stochastic nature of the avalanche breakdown is well known [11]. It leads to a large spreading of the time of detection and to the concept of probability P_A of avalanche breakdown. Here, for $V_{BIAS} = 11$ V, we have

obtained $P_A \approx 82\%$, independently of the quenching circuit parameters. An avalanche time T_A can be defined as the time needed for the avalanche breakdown current to reach the value $I_{BD} = 5 \mu\text{A}$ after photon absorption.

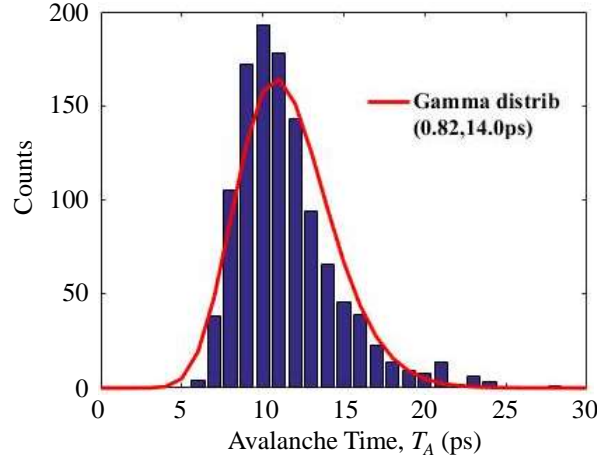


Figure 3. Histogram of avalanche time for a set of 1157 simulations with random energy-wave vector coordinates of initial e-h pair and different values of R_Q and C_Q ($V_{BIAS} = 18 \text{ V}$).

The histogram of 1157 values plotted in Fig. 3 exhibits a quite large spreading around the average value $\langle T_A \rangle = 11.5 \text{ ps}$ with a standard deviation of 3.08 ps . It should be noted that this average value and this spreading describe only the intrinsic part the avalanche stochasticity due to the random nature of the energy-momentum coordinates of the initial e/h pair generated by the photon absorption. Indeed, the position of the photon absorption was always the same, i.e. in the center of the high-field region of the device. The contribution of the randomness of the initial e/h pair position is not included in this statistics. The histogram of Fig. 3 can be fitted by a gamma distribution with parameters $k = 0.82$ and $\theta = 14.0 \text{ ps}$.

Importantly, the quenching process also appears to have a strong probabilistic character, as previously observed for a Si device [4]. In Fig. 4, we plot the time response of the current through the SPAD and the intrinsic SPAD voltage after an electron/hole (e/h) pair generation by photon absorption at $t = 0$ in the center of the device for three simulations corresponding to three different random selections of the energy and wave vector coordinates of the initial e/h pair.

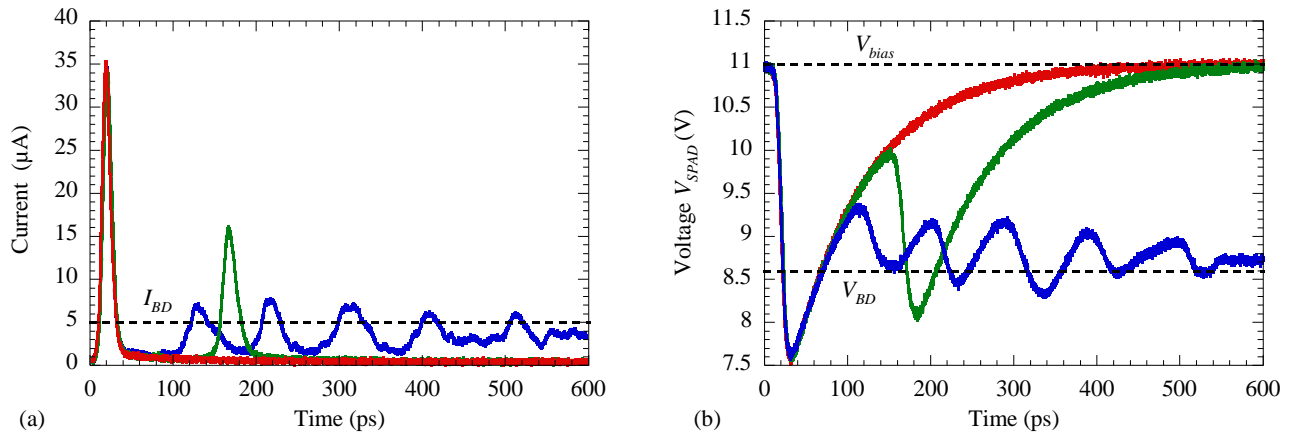


Figure 4. Time evolution of (a) current and (b) SPAD voltage for initial e-h pair generated at $t = 0 \text{ s}$ with $R_Q = 700 \text{ k}\Omega$, $C_Q = 0.1 \text{ fF}$, $V_{BIAS} = 11 \text{ V}$. Each color corresponds to a random set of energy-wave vector coordinates of initial e-h pair. The horizontal dashed lines represent the breakdown detection current I_{BD} , the bias voltage V_{BIAS} and the breakdown voltage V_{BD} .

Starting from $V_{SPAD} = V_{BIAS}$, we observe either a single avalanche followed by the quenching with return to initial state (red), a double-avalanche with quenching (green), or no quenching at all (blue) with a final V_{SPAD}

close to V_{BD} . In terms of current, the main avalanche peak is similar for the three cases but it may be followed by a secondary peak (double avalanche) before the current vanishes close to zero. In case of no quench (blue curve), we observe several peaks of current that oscillates around I_{BD} without vanishing. All these parasitic peaks can be understood by the system as the detection of a photon absorption though only a single photon was actually absorbed.

The quenching probability P_Q is obviously strongly dependent on the parameters R_Q and C_Q of the quenching circuit. Figure 5a shows the influence of the resistance R_Q on the probability P_Q at given values of C_Q . Beyond a threshold resistance value that depends on C_Q , P_Q increases rapidly from 0 to 100%. This simple behavior is easy to understand as a consequence of the increase of the time of discharge $\tau = R_Q C_Q$ of the capacitance that increases the chance to fully evacuate all excess carriers generated by the avalanche, and thus to prevent the triggering of new impact ionizations by remaining particles. The same behavior was observed in the Si device [4], as shown in dashed line for comparison.

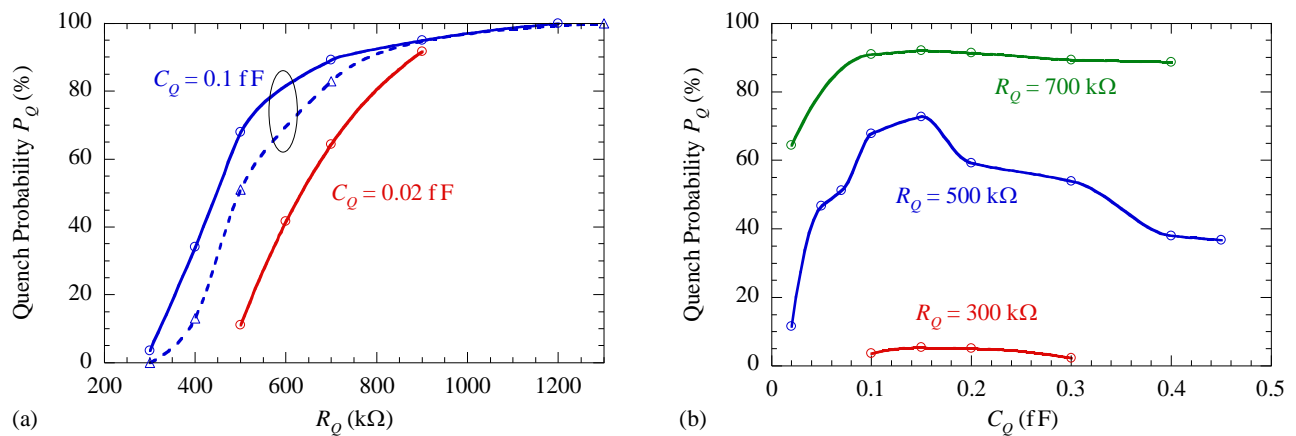


Figure 5. Quenching probability as a function of (a) the resistances R_Q and (b) the capacitance C_Q ($V_{BIAS} = 11$ V). Dashed line in (a): results obtained for the Si device [4] with $V_{BIAS} = 18$ V.

The influence of C_Q on the quenching probability P_Q is more complicate to analyze due to the fact that two antagonistic phenomena are in competition. The increase of C_Q tends to increase the time of discharge τ , which is likely to enhance P_Q , but it also increases the amount of excess charges generated by the avalanche and stored in the capacitance, which makes the quenching more difficult. As a result of this competition, we observe in Fig. 5b that at low (high) R_Q the probability P_Q is low (high) and weakly dependent on C_Q , and that for intermediate resistance $R_Q = 500$ k Ω the evolution of P_Q as a function of C_Q is quite erratic, though it presents a maximum for $C_Q = 0.15$ fF, as for all values of R_Q . This non trivial behavior requires further analysis to be fully understood quantitatively.

5. Conclusion

We have analyzed the statistical behavior of a Ge SPAD using 3D self-consistent Monte Carlo simulation and shown in particular the probabilistic character of the quenching operation. The quenching resistance has a strong effect on the quenching probability that can rapidly switch from 0 to 100% according to this parameter. The effect of the quenching capacitance is more subtle due to the competition between two antagonistic phenomena (excess charge and discharge time) that makes its quantitative influence difficult to predict in the case of intermediate values of quenching resistance. The 3D Monte Carlo method appears to be very convenient to capture the effects of all stochastic ingredients of SPAD operation.

Acknowledgements

Financial support from the ANR project “GeSPAD” (ANR-20-CE24-0004) and the “Nano2022” project under the IPCEI program is gratefully acknowledged.

References

- [1] S. Cova, M. Ghioni, A. Lacaita, C. Samori, and F. Zappa, "Avalanche photodiodes and quenching circuits for single-photon detection", *Appl. Optics*, vol. 35 (12), pp. 1956-1976, 1996.
- [2] F. Zappa, A. Tosi, A. DallaMora, and S. Tisa, "SPICE modeling of single photon avalanche diodes", *Sensors and Actuators A: Physical*, 153 (2), pp. 197-204, 2009.
- [3] Y. Oussaiti, D. Rideau, J. R. Manouvrier, V. Quenette, B. Mamdy, C. Buj, J. Grebot, H. Wehbe-Alaouse, A. Lopez, G. Mugny, M. Agnew, E. Lacombe, M. Pala and P. Dollfus, "Verilog-A model for avalanche dynamics and quenching in Single-Photon Avalanche Diodes", in *Proc. SISPAD*, 2020, pp. 145–148.
- [4] T. Cazimajou, M. Pala, J. Saint-Martin, R. Helleboid, J. Grebot, D. Rideau, and P. Dollfus, "Quenching Statistics of Silicon Single Photon Avalanche Diodes", *J. Electron Devices Society*, vol. 9, pp. 1098-1102, 2021.
- [5] P. Dollfus, A. Bournel, S. Galdin-Retailleau, S. Barraud, and P. Hesto, "“Effect of discrete impurities on electron transport in ultra-short MOSFET using 3D Monte Carlo simulation”, *IEEE Trans. Electron Devices*, vol. 51, no. 5, pp. 749–756, 2004.
- [6] V. Aubry-Fortuna and P. Dollfus, "Electron transport properties in high-purity Ge down to cryogenic temperatures", *J. Appl. Phys.*, vol. 108, 123706, 2010.
- [7] M. V. Fischetti and S. E. Laux, "Band structure, deformation potentials, and carrier mobility in strained Si, Ge, and SiGe alloys", *J. Appl. Phys.*, vol. 80, pp. 2234-2252, 1996.
- [8] Y. Kamakura, H. Mizuno, M. Yamaji, M. Morifuji, K. Taniguchi, C. Hamaguchi, T. Kunikiyo, and M. Takenaka, "Impact ionization model for full band Monte Carlo simulation", *J. Appl. Phys.*, vol. 75, pp. 3500-3506, 1994.
- [9] T. Mikawa, S. Kagawa, T. Kaneda, and Y. Toyama, "Crystal orientation dependence of ionization rates in germanium", *Appl. Phys. Lett.*, vol. 37, pp. 387-389, 1980.
- [10] S. Babiker, A. Asenov, N. Cameron, S. P. Beaumont, and J. R. Barker, "Complete Monte Carlo RF analysis of ‘real’ short-channel compound FET’s", *IEEE Trans. Electron Devices*, vol. 45, no. 8, pp. 1644–1652, 1998.
- [11] D. Dolgos, H. Meier, A. Schenk, and B. Witzigmann, "Full-band Monte Carlo simulation of high-energy carrier transport in single photon avalanche diodes: Computation of breakdown probability, time to avalanche breakdown, and jitter", *J. Appl. Phys.*, vol. 110, 084507, 2011.